Quantitative live-cell analysis of microtubule-uncoupled cargo-protein sorting in the ER

Anna Dukhovny, Andreas Papadopulos and Koret Hirschberg*

Department of Pathology, Sackler School of Medicine, Tel-Aviv University, Tel-Aviv 69978, Israel

*Author for correspondence (e-mail: koty@post.tau.ac.il)

Accepted 11 December 2007
J. Cell Sci. 121, 865-876 Published by The Company of Biologists 2008
doi:10.1242/jcs.019463

Summary

The sorting and concentration of cargo proteins within ER exit sites (ERESs) is a fundamental function of the secretory machinery. The mechanism by which peripheral coat complexes and their small GTPase effectors mediate this function with export membrane domains is only partially understood. The secretory-machinery-mediated sorting to ERESs is a process that counters the entropy-driven even distribution of membrane proteins within organellar membranes. Here, for the first time, we quantified the dynamic properties of GFP-VSVG sorting to ERESs in living cells by uncoupling it from later translocation steps using microtubule depolymerization. The dynamics of the ER to ERES redistribution of cargo proteins was quantified in single cells by measuring changes in fluorescence-intensity variance after shift to the permissive temperature. Cargo concentration within ERESs continued in cells overexpressing the GTP-locked ARF1Q71L or in the presence of brefeldin A. In the absence of COPI and microtubules, ERESs transformed from tubulovesicular to spherical membranes that actively accumulated secretory cargo and excluded ER-membrane markers. We found sorting to ERESs to be a slow and diffusion-unlimited process. Our findings exclude COPI, and identify the COPII protein complex to be directly involved in the secretory cargo sorting and redistribution functions of ERESs.

Supplementary material available online at
http://jcs.biologists.org/cgi/content/full/121/6/865/DC1

Key words: Endoplasmic reticulum, ER-exit sites, sorting, secretory pathway, membrane, live-cell imaging, COPII, COPI

Introduction

The secretory pathway is comprised of membrane-bound organelles, each defined by a unique composition of proteins and lipids that serve a distinct set of functions. These organelles exchange molecules via tubular-vesicular membrane carriers (VTCs) that translocate across the cytosol on microtubule tracks. The secretory pathway is comprised of the ER, the Golgi complex and the plasma membrane. The first sorting station for correctly folded proteins in the secretory pathway is the ER exit site (ERES) (Mezzacasa and Helenius, 2002), also called transitional ER. This pleiomorphic membrane domain is continuous with the rest of the ER membrane and is associated with the export of secretory cargo (Ward et al., 2001). ERES membranes are identified by the presence of the COPII protein complex (Hobman et al., 1998; Tang et al., 2005). Formation of this complex is initiated with the recruitment of the small GTPase Sar1 by the Sec12 transmembrane protein. Sar1, in its membrane-associated, GTP-bound form, sequentially recruits cargo proteins and the heterodimers Sec23/24 and Sec13/31. This dynamic outer shell of the COPII coat complex has been shown to interact with targeting signals of cargo proteins (Votsmeier and Gallwitz, 2001), as well as to affect various features of the membrane, such as curvature and possibly lipid composition (Graham, 2004). There are two main hypotheses regarding the role and localization of the COPII complex during ER export. The first (Fromme and Schekman, 2005) suggests that COPII is involved in multiple transport stages from cargo recruitment to the formation of COPII-coated vesicles. One prediction of this theory is a model in which COPI is involved with transport in the opposite direction, namely from the Golgi to the ER. The second hypothesis, according to Luini and colleagues (Mironov et al., 2003), states that COPII localizes to a domain within the ERES in which cargo in the ERES is found segregated from the COPII coat complex and budding transport intermediates do not contain COPII.

The COPI coat complex and its ARF1 effector are also essential for protein export from the ER (Ward et al., 2001), as has been principally demonstrated by the complete blockage of ER export by the drug brefeldin A (BFA) (Barzilay et al., 2005; Sciaky et al., 1997). Thus, the actual sorting and concentration of cargo proteins in ERESs is presumed to be driven by more than one type of interaction. Binding of the COPII Sec24 to the DXE acidic motifs in the cytosolic tail of integral membrane proteins has been demonstrated, although only weak interactions were reported (Miller et al., 2003; Mossessova et al., 2003). The role of membrane curvature, thickness and lipid composition in the sorting process has not been fully addressed in this context. However, several lines of evidence strongly support the hypothesis of a role for ERES membrane lipids in cargo sorting and concentration. One obvious observation is that the ERES membranes are highly curved, tubular-vesicular structures (Balch et al., 1994), in contrast to ER membranes, which are either reticular or flat cisternal (Voeltz et al., 2002). In addition, cholesterol has recently been demonstrated to be important for ER export (Ridsdale et al., 2006). Finally, membrane curvature has been associated with the binding of COPII coat complexes (Antonny, 2006). This result can be interpreted as induction of vesicle formation or simply, membrane curvature.

The absence of intracellular microtubule tracks affects, but does not block, ER-to-Golgi transport: cargo proteins as well as recycling Golgi proteins are sorted and concentrated in the ERESs. The Golgi complex redistributes to form functional single Golgi stacks adjacent to each ERES (Cole et al., 1996) and the cargo proteins are processed

and moved through these organelles to arrive at the plasma membrane (Presley et al., 1997).

In this study, we use the fluorescently tagged tsO45 thermoreversible mutant of vesicular stomatitis virus G protein (VSVG-FP). VSVG-FP has been extensively used as a reporter to address dynamic properties of secretory membrane transport in living cells (Lippincott-Schwartz et al., 2000; Presley et al., 1997; Vasserman et al., 2006). In the absence of polymerized microtubules, VSVG is sorted and concentrated in the ERES after a shift to permissive temperature. The kinetic properties of this sorting process were analyzed by following the temporal change in the variance of pixel fluorescence intensity. We found that the redistribution of VSVG-FP from ER to ERESs is a relatively slow process that is not limited by diffusion. We also found that accumulation of cargo within ERESs coincides with an increase in the recruitment of at least one of the COPII components (Sec31) to ERES membranes. Using the ARF1 GTP-bound, membrane-locked mutant Q71L and BFA, we found that early cargo sorting and concentration within ERESs occur independently of ARF1 and the COPI protein coat. However, in the absence of COPI and microtubules, the pleiomorphic tubulovesicular ERESs transformed to dilated spherical membranes, which specifically accumulated secretory cargo proteins, excluded an ER-membrane marker, as well as a mutated VSVG-FP without the acidic motif, and were unstable, because they occasionally re-fused with ER membranes. Moreover, COPII protein complex localized to a distinct pole within these membrane structures. These data allow us to assign specific roles for the sequential function of COPII and COPI in ER export.

Results

Characterization of VSVG transport in the absence of microtubules

In this study, we focused on the early step of membrane cargo sorting and concentration in the ERESs. Sorting to the ERESs is defined as an energy-requiring process, mediated by the secretory-machinery proteins, which results in the redistribution and concentration of specific membrane cargo proteins in those sites. A major obstacle in the ability to measure cargo sorting is the fact that sorting to ERESs is constantly interrupted by the subsequent budding and translocation along microtubule tracks to the Golgi complex. Thus, a sorted cargo mass is not accumulated but rather constantly conveyed to the perinuclear region. To study cargo-sorting dynamics in isolation, the cargo-sorting process was uncoupled from the subsequent translocation steps by depolymerizing the microtubules. This was achieved by the addition of nocodazole (NOC) to the cell medium during a 20-minute incubation of the cells on ice. In COS7 cells, trafficking of VSVG from the ER to the plasma membrane persists in the absence of microtubules (Hirschberg et al., 1998; Rogalski et al., 1984; Storrie et al., 1998). However, the morphology and distribution of the secretory organelles and transport intermediates, as well as the trafficking dynamics, change significantly. One of the major outcomes of microtubule depolymerization is the redistribution of the Golgi from the microtubule-organizing center to scattered yet functional stacked cisternae called Golgi mini-stacks (Cole et al., 1996). It has been demonstrated that upon microtubule depolymerization, Golgi membranes recycle through the ER and emerge from ERESs to form numerous functional Golgi units in the form of a single stack of cisternae. We then sought to characterize the dynamics of this NOC-mediated process of Golgi redistribution. In particular, we were interested in analyzing this process during ER export of the fluorescently tagged membrane cargo VSVG-FP. The VSVG-CFP membrane cargo protein was coexpressed in COS7 cells with the Golgi marker YFP-GalT. Cells were transferred to ice after being held overnight at 40°C. After a 20-minute incubation on ice in the presence of NOC, cells were imaged at the permissive temperature by confocal microscopy. The representative images in Fig. 1A demonstrate the redistribution of the Golgi occurring in conjunction with ER-to-ERES sorting of VSVG-FP. The rate of redistribution of the perinuclear Golgi was analyzed by measuring the fluorescence intensity in the Golgi region. Fitting to a simple exponential, we found the time constant of the redistribution of the central Golgi-associated fluorescence to be approximately 80 minutes (Fig. 1B). We then sought to quantify the concomitant appearance of GalT in peripheral structures, as well as to compare it with that of VSVG-FP sorting. The appearance of both VSVG and GalT in ERESs was quantified by analyzing the variance of the pixel fluorescence intensity in a region of interest (ROI) at the periphery of the cell that excluded the central Golgi structure (Fig. 1C). As further detailed below, the variance expresses the averaged distribution of pixel intensities relative to the mean intensity of the ROI. Thus, its values increase as molecules change their distribution from homogeneous within the ER to clustered in the ERESs. This was necessary for appropriate comparison of the distribution of the incoming and redistributing Golgi marker with that of the ER-resident exported VSVG-FP. The appearance of GalT and VSVG in peripheral structures was nearly simultaneous, with that of GalT being somewhat slower and limited in distribution to the vicinity of the original microtubule-organizing center (Fig. 1A). These data demonstrate that upon arrival at the ER, GalT is a bona fide cargo, as is the folded VSVG.

To further characterize the secretory transport of VSVG in the absence of NOC, the VSVG-FP membrane cargo protein was coexpressed in COS7 cells with CFP-tagged Srβ (Fig. 2A) or Sec31 (Fig. 2B), markers of ER membranes and ERESs, respectively. Cells were fixed at various times after being shifted to the permissive temperature (34°C, Fig. 2A,B) and confocal images of representative cells were obtained. In Fig. 2A, the redistribution of VSVG-FP is demonstrated by comparison to the distribution of the ER-membrane marker Srβ-CFP. Interestingly, we found that during incubation in the absence of microtubules, the morphology of the ER membranes changed from tubular-reticular to flat (Fig. 2A lower panel, 0 and 30 minutes). At longer incubations (≈4-5 hours), the ER collapses into the perinuclear region (Fig. 2A lower panel, 300 minutes). Upon shift to the permissive temperature, redistribution of VSVG-FP from ER membranes to the typically punctate ERESs was clearly observed. Sec31 is a peripheral membrane component of the COPII coat protein and is a bona fide marker of ERESs. As VSVG arrived from the ER, it colocalized with Sec31 (Fig. 2B, 30 minutes). At later time points after the shift (Fig. 2B, 120 minutes), the VSVG-FP localized with, but was completely segregated from the Sec31-CFP marker. Consequently, Figs 1 and 2 demonstrate that in the absence of microtubule-mediated translocation in the cell, secretory transport of the VSVG-FP membrane cargo proceeds all the way to the plasma membrane.

Quantitative analysis of the dynamics of ER-to-ERES sorting

We applied a novel quantitative approach to analyze the robust change in distribution of VSVG-FP as it is sorted from the ER to the ERESs. At the single-cell level, a direct quantification of this process via analysis of changes in fluorescence intensity is technically difficult because the ERESs are small dynamic structures

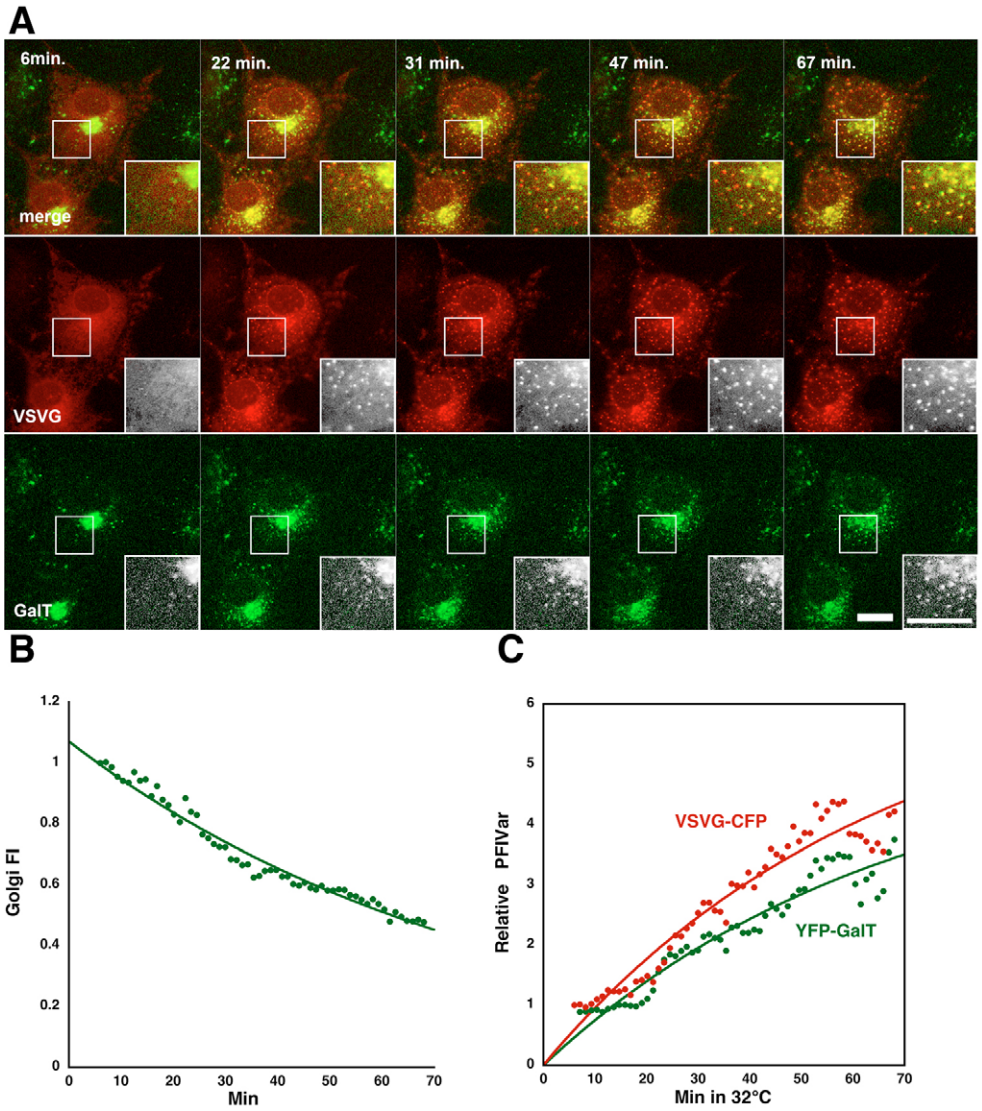

Fig. 1. ER export of VSVG-FP and Golgi redistribution upon microtubule depolymerization. (A) Confocal images of living COS7 cells coexpressing GalT-YFP (green) and VSVG-CFP (red). For complete microtubule depolymerization, cells were transferred to ice for 20 minutes following a 24 hour incubation at the nonpermissive temperature (40°C) to accumulate VSVG in the ER. Nocodazole (1 μg/ml) was added and images of the cells at the permissive temperature (34°C) were captured for the indicated times. Inserts are enlarged twofold to show the appearance of GalT-YFP and VSVG-CFP in the ER exit sites. Scale bars: 10 μm. (B) Quantitative analysis of the time-dependent decrease in fluorescence intensity (FI) in a region of interest over the Golgi complex of the top cell in A. The line is a simple exponential fit with a rate of 1.23% per minute (R^2=0.97). (C) Analysis of the ER export of VSVG-CFP and GalT-YFP in nocodazole-treated cells. Graph shows the time-dependent relative change in variance of fluorescence intensity in a region of interest over the cell in an area that excludes the pre-redistributed Golgi complex.

that are spread throughout the ER. In addition, when VSVG-FP-expressing cells are shifted to the permissive temperature, the fluorescence intensity of the ERESs increases while that of the background ER decreases. Moreover, analysis in a single cell of the change in total or average fluorescence intensity with time during sorting of VSVG-FP from ER to ERESs does not provide any information on the sorting process, namely the time-dependent redistribution of the VSVG-FP. Therefore, to capture the secretory-machinery-mediated change in distribution of VSVG in the ER membrane, we analyzed the temporal change in the variance of pixel fluorescence intensity (PFIVar). The rationale was that at non-permissive temperatures, VSVG-FP is evenly distributed within the ER, resulting in low initial PFIVar values. As VSVG is sorted to the ERESs, the fluorescence intensity of the ER is reduced while that of the ERESs increases. This is reflected by an increase in PFIVar that depicts the deviation from the constant average fluorescence-intensity values in the analyzed ROI (Fig. S1 in supplementary material). A major advantage of variance is the ease with which this information can be collected using any commercial or freeware image-processing software such as NIH Image and Image J (Wayne Rasband, NIH, MD). Fig. 3 demonstrates a typical quantification of the sorting of VSVG-FP to ERESs during a 45-minute period after the shift to the permissive temperature in living cells. The sorting and concentration in the ERESs is shown in Fig. 3A (see also corresponding supplementary material Movie 1). In Fig. 3B, the normalized change in PFIVar is plotted against time for two typical cells. The data were fitted to an exponential growth equation and yielded time constants (inverse of the rate coefficients of the exponential equation) of 20.2±1.8 and 25.0±2.8 minutes for cells A and B, respectively. To further demonstrate the direct association between the sorting dynamics and the PFIVar values, we analyzed the process at the two permissive temperatures, 34°C and 18°C (Mezzacasa and Helenius, 2002). The time constants for fitting the average change in PFIVar for 12 and 14 cells to an exponential equation were 27.5 and 107.7 minutes for 34°C and 18°C, respectively (Fig. S2 in supplementary material). In Fig. 3C, the sorting and concentration of VSVG-FP in a single ERES were followed in a living cell (see also supplementary material Movie 2). Analyses of the time-dependent change in the average fluorescence intensity in a typical single ERES, as well as normalized and averaged data for 10 ERESs, are shown in Fig. 3D. The data were best fitted to a sigmoid equation, as the rate of

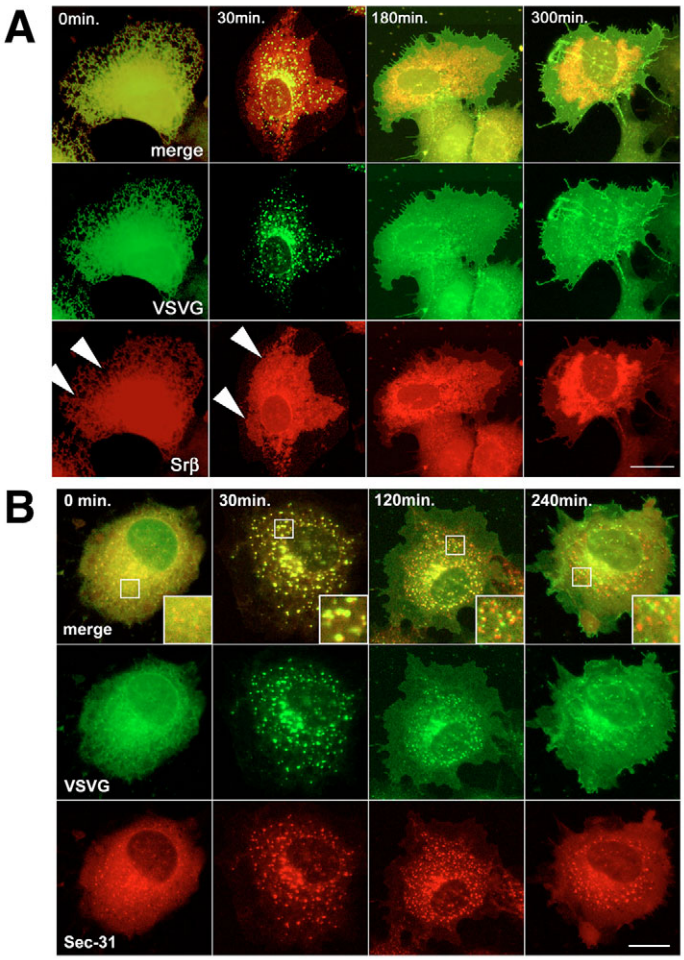

Fig. 2. Secretory traffic of VSVG-FP in the absence of microtubules. Confocal images of fixed COS7 cells coexpressing VSVG-YFP (green, A-B) and either the ER marker Srβ-CFP (A, red) or the ER exit site marker Sec31-CFP (B, red). For complete microtubule depolymerization, cells were transferred to ice for 20 minutes following a 24 hour incubation at the nonpermissive temperature (40°C) to accumulate VSVG in the ER. Nocodazole (1 μg/ml) was added and the cells were incubated at the permissive temperature (34°C) for the indicated times before addition of formaldehyde. Arrowheads indicate reticular and flat ER membranes. Scale bars: 10 μm.

fluorescence accumulation in the ERES increased and then decreased to apparent saturation. This saturation presumably reflects the transport of VSVG-FP through the superimposed post-ERES compartments. The data collected from a single ERES demonstrate composite kinetics of the sorting and accumulation of VSVG in ERESs.

Thus, we found the rate constant for sorting at physiological temperature to be 3.64±0.07% per minute (27.5 minute time constant). These values imply that the redistribution of VSVG to ERESs is noticeably slow compared with the fast diffusional mobility reported for VSVG in the ER membrane (D=0.45 μm^2/second) (Nehls et al., 2000). The fact that the ER-membrane morphology changes in the absence of microtubules from reticular to mostly flat (Fig. 2A, 0 and 30 minutes) allowed us to perform FRAP experiments and obtain the diffusion coefficient (D) value for VSVG-FP in ER membranes in our system (NOC-treated cells) (Siggia et al., 2000) (Fig. 4C). The recovery data were fitted to the equation described in the Materials and Methods, yielding D=0.42±0.02 μm^2/second (n=4), which is comparable with previously reported values. Thus, the time constant for diffusion of VSVG-FP through the estimated area surrounding an ERES (≈10 μm^2) is 24 seconds. This value is over 60-fold faster than the time constant measured for the sorting process (27.5 minutes). A slow net flux of VSVG-FP moving from the ER to ERESs can be simply explained by the fact that VSVG efficiently recycles back from the peripheral VTCs or Golgi mini-stacks. It has previously been suggested that Golgi-to-ER retrograde transport is microtubule independent (Sciaky et al., 1997). Thus, the increased retrograde transport facilitated by the close proximity of ERES VTCs and Golgi mini-stacks and the slowed microtubule-dependent anterograde transport are both plausible explanations for the NOC-mediated reduction in the speed of VSVG-FP secretory transport. To demonstrate the existence of a significant reverse flux from the ERES and associated Golgi mini-stacks back to ER membranes, NOC-treated cells were shifted to the permissive temperature for 25 minutes and a ROI including most of the VSVG-FP in the ER and ERESs was photobleached, except for a small area, as shown in Fig. 4A (see also supplementary material Movie 3). The fluorescence intensity of the unbleached ROI then decreased while ERESs in the bleached ROIs reappeared. A simple two-compartment model (compartments representing the ER between unbleached and bleached ERESs/VTCs/Golgi mini-stacks were excluded because the fluorescence-intensity values of VSVG-FP when in the ER were very low) was used to simulate the movement from unbleached to bleached ERESs via the ER during the last 10 minutes of the recovery, in order to minimize the contribution of the initial diffusion of unbleached VSVG-FP that was still in the ER membranes (Fig. 4B). Because protein-synthesis inhibitors were not used, we determined the possible contribution of de novo synthesis or folding of the fluorescent moiety by plotting the time-dependent changes in total fluorescence intensity of the cell (Fig. 4B insert). A fit to a linear equation yielded a minor slope of fluorescence-intensity increase (only 0.23% per minute). The rate constant for movement from unbleached to bleached ERESs was 4% per minute. These observations suggest that at permissive temperatures, there is significant recycling of VSVG-FP molecules from secretory compartments distal to the ERESs back to the ER.

Sorting and COPII coat proteins

The COPII protein complex has been demonstrated to bind exported cargo proteins (Votsmeier and Gallwitz, 2001), which in turn affect its membrane recycling dynamics (Forster et al., 2006). Thus, we asked whether we could detect these interactions in our experimental system, which lacks polymerized microtubules (Guo and Linstedt, 2006; Watson et al., 2005). In addition, the co-incidence of VSVG-FP concentration in the ERESs with increased recruitment of COPII proteins could conceivably explain the non-linear sorting kinetics observed at the level of a single ERES. Fig. 5 demonstrates dual-color live-cell analysis of cells coexpressing VSVG-FP and Sec31-CFP. The images (and supplementary material Movie 4) show a clear increase in membrane-bound Sec31 during ER-to-ERES sorting of the VSVG-FP. To compare the sorting of VSVG-FP to the recruitment of cytosolic Sec31-CFP, we analyzed the change in PFIVar for both proteins (Fig. 5B). In this case, for the Sec31-CFP, the increase in variance values signified a net recruitment from the cytosol to the ERES membranes. The increases in variance values, fitted to a simple exponential, were 6.4 and 1.65% per minute for VSVG-FP and Sec31-CFP, respectively. The rate of increase in

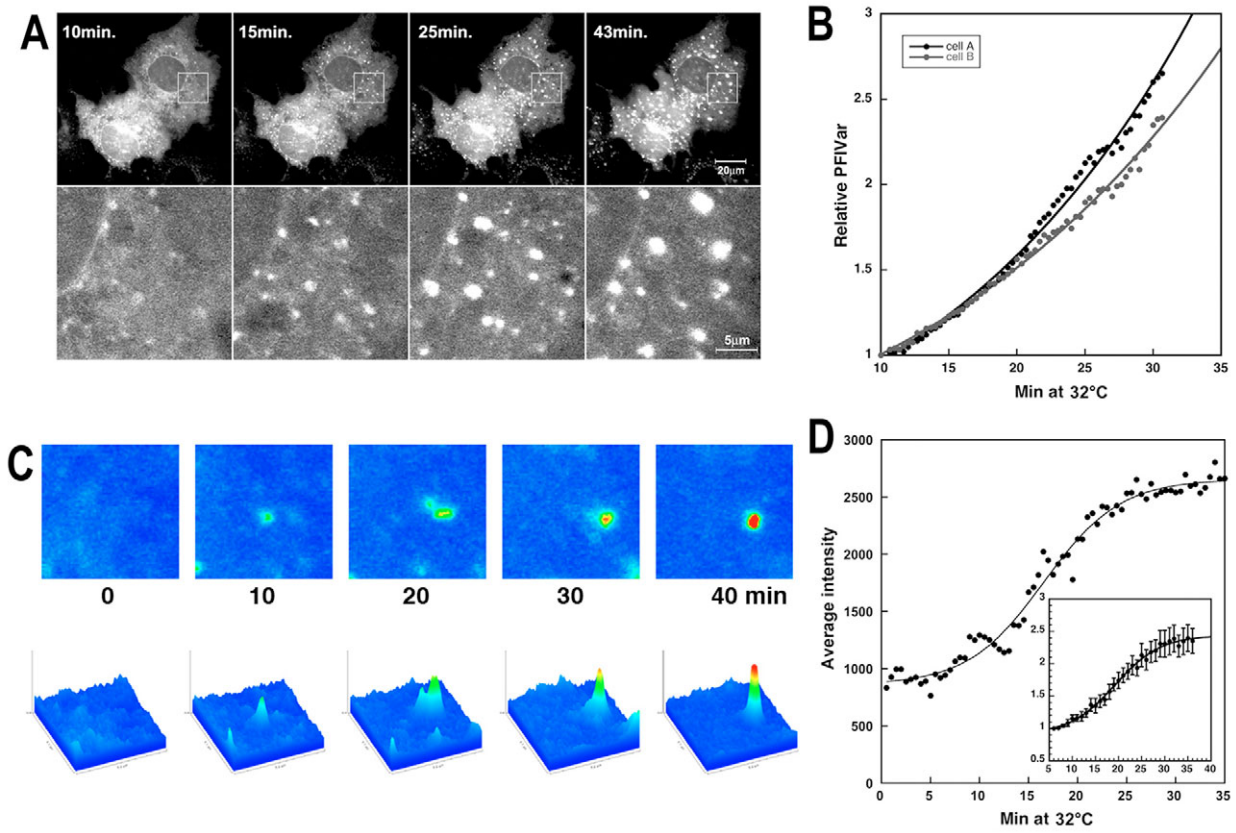

Fig. 3. Analysis of ER-to-ER exit site (ERES) sorting of VSVG-FP. (A) VSVG-GFP-expressing COS7 cells were incubated for 24 hours at the nonpermissive temperature (40°C) to accumulate VSVG in the ER. Cells were then transferred to ice for 20 minutes and 1 μg/ml nocodazole was added before an additional 20-minute incubation at 40°C. Image analysis was initiated upon transfer of the cells to the permissive temperature (34°C). Images were captured at 20-second intervals. Lower panels, 4× enlarged inserts to show the accumulation in ERESs (see also supplementary material Movie 1). (B) Time-dependent increase in relative PFIVar, calculated as described in the Materials and Methods (black and gray circles) for two representative cells. Data were fitted to an exponential equation ($y = ae^{kx}$) (lines). R^2 values were 0.99 for both data sets, k values were 0.0494 second^{-1} and 0.0409 second^{-1}. (C) Pseudocolor images (upper panel) and surface-plot (lower panel) of a single ERES during cargo sorting (see also corresponding supplementary material Movie 2). (D) Time-dependent increase in average fluorescence intensity of a region of interest within a single ERES, calculated as described in Materials and Methods (black full circles) for a representative ERES. Data were fitted to the sigmoid equation y=864+(1796/(1+e$^{4.25-0.26x}$) (lines). R^2 value is 0.98. Insert is a plot of normalized and averaged data from 10 cells. Error bars indicate s.e.m.

ERES-membrane-bound Sec31-CFP was significantly slower than that of the cargo VSVG-FP, suggesting a complex relationship between cargo accumulation and COPII recruitment.

Sorting and COPI coat proteins

As ARF1 and the COPI complex are also associated with ER-to-Golgi transport (Dascher and Balch, 1994; Ward et al., 2001), we asked whether the ARF1 small GTPase and its associated COPI coat complex are essential for cargo sorting and concentration. Coexpression of ARF1-CFP with VSVG-FP demonstrated visible localization of ARF1 to the ERESs in NOC-treated cells only after redistribution of the Golgi complex (Fig. 6A). The constitutively GTP-bound Q71L mutant of ARF1 is locked on the Golgi and ERES membranes (Presley et al., 2002; Ward et al., 2001). In cells overexpressing ARFQ71L-CFP, secretory traffic is blocked. The GTP-bound mutant Q71L tagged with CFP (ARFQ71L-CFP) was coexpressed with VSVG-FP. NOC treatment resulted in slower redistribution of the membrane-bound protein to peripheral punctate structures. However, after the shift to permissive temperatures, VSVG was redistributed and concentrated in the ERESs, even though further transport beyond the ERESs to the plasma membrane was completely blocked (Fig. 6B). FRAP analysis of cells coexpressing ARFQ71L-CFP and VSVG-FP clearly demonstrated that VSVG-FP is irreversibly localized with the membrane-locked ARFQ71L-CFP (Fig. S3 in supplementary material). A possible interpretation is that ARFQ71L-CFP labels post-ERES membranes and thus retrograde transport is blocked. To eliminate the possibility that endogenous ARF1 and thus COPI dynamics are responsible for the sorting activity, BFA was added to NOC-treated VSVG-FP and ARFQ71L-CFP coexpressing cells (data not shown). The BFA was intended to strip the ER and related membranes of endogenous cycling ARF1 and COPI complexes. In the presence of BFA, in ARF1Q71L-CFP-expressing cells, VSVG-FP was still sorted and concentrated within peripheral punctate structures. These data can be interpreted in two ways: the first is that ARF1 and COPI dynamics, namely their cytosol-ERES membrane exchange, are not directly required for the sorting and concentration of VSVG-FP cargo but rather for later stages of ER export; the second interpretation is that the membrane-bound form of ARF1 is sufficient to facilitate the sorting process. The later transport steps, which are blocked, probably require the on-off GTPase-cycle-controlled shuttling of ARF1 and COPI.

To distinguish between these two hypotheses, we shifted VSVG-FP-expressing cells to the permissive temperature after

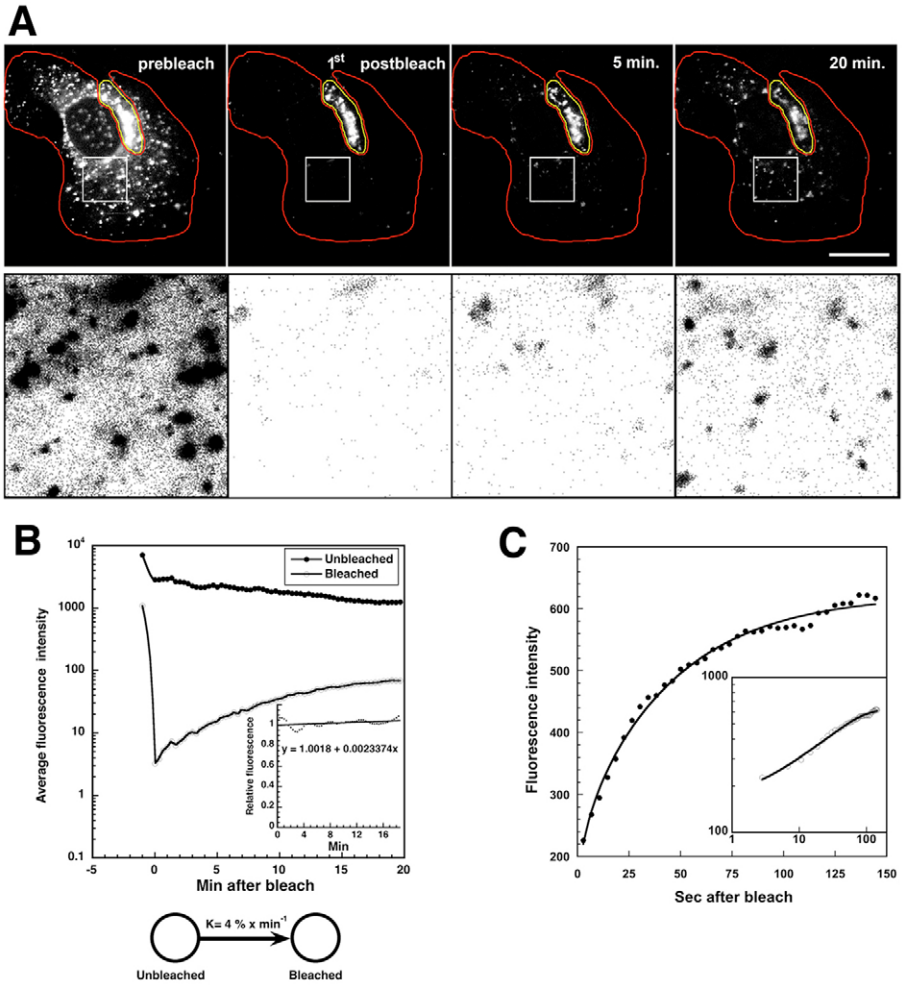

Fig. 4. FRAP analysis of VSVG diffusion and reverse ER exit site-to-ER flux. (A) Cells expressing VSVG-GFP were treated with nocodazole as described previously. 25 minutes after shift to the permissive temperature, most of the cell was photobleached, apart from the area circled in yellow. Images were captured at 20-second intervals for an additional 20 minutes. Lower panel, inverted and magnified images of the boxed areas in the upper panel (see also corresponding supplementary material Movie 3). Scale bar: 10 μm. (B) Quantitative analysis of the average and total (insert) fluorescence intensities of the bleached (open circles) and unbleached (closed circles) regions of interest. Lines in the insert were generated by simulation using SAAM II software. The simple model used is illustrated below the graph. The rate constant obtained from the fit is 4% per minute. Insert was fitted to a linear equation (continuous line) indicating an increase in total fluorescence intensity of 0.23% per minute. (C) FRAP analysis of VSVG-GFP in the ER of nocodazole-treated COS7 cells. The rectangle photobleaching, image acquisition and extraction of the apparent diffusion coefficient are described in the Materials and Methods. Insert is a full-log-scale graph to show the quality of fit at all time points.

microtubule depolymerization in the presence of BFA. As shown in Fig. 7A, during the first 30-45 minutes after the shift, VSVG-FP was observed localizing and concentrating into a population of rather uniform and spherical membrane structures that were dispersed throughout the cell. These dilated membrane spheres were unstable, as they occasionally fused with each other or disappeared by fusing with and dissipating into the ER membranes (Fig. 7A and supplementary material Movie 5). This instability of the cargo-containing membranes probably reflects the apparent slow (0.74% per minute) and ineffective sorting measured by the time-based change in PFIVar (Fig. 7B). Addition of BFA to VSVG-FP-labeled ERESs at 10-15 minutes after the shift to the permissive temperature confirmed that the spherical membranes originate directly from the ERESs (Fig. 7C and supplementary material Movie 6). Interestingly, after addition of BFA, VSVG-FP did not disperse back into the ER but remained concentrated within these membranes as they transformed into spherical membranes. A three-dimensional reconstruction of a single VSVG-FP-labeled spherical membrane is shown in Fig. 7D. The dimensions of such spherical membranes are presented in Table 1. FRAP analysis of cells expressing both CFP- and YFP-tagged VSVG demonstrated that VSVG constantly accumulates in the spherical BFA-induced ERESs membranes (Fig. S4 in supplementary material). Analysis of the average fluorescence intensity of single dilated ERESs demonstrated that they go through cycles of actively accumulating VSVG followed by rapid collapse. The lifetime through two such cargo concentration cycles is shown in Fig. 7E. Analysis of the accumulation of VSVG inside the spherical membranes demonstrated a sorting rate of approximately 5% per minute, which is comparable with the apparent sorting rate observed without BFA. The first sorting cycle of the dilated ERES analyzed in Fig. 7E is shown in the pseudocolor surface plot in Fig. 7F. These data lend support to the hypothesis that COPII complex is involved in cargo sorting. Moreover, COPII can mediate cargo sorting of VSVG-FP at normal rates in the absence of COPI, ARF1 and polymerized microtubules. The lifetime of the spherical ERESs was highly variable, ranging between 8 and 25 minutes. Their collapse was reminiscent of BFA-mediated Golgi blink-out, especially since occasional tubular membranes could be visualized emanating from them prior to their collapse (data not shown). That the collapse occurred back into the ER is confirmed by the observation that even after long incubations (over 3 hours, data not shown) at the permissive temperature, VSVG was exclusively localized to the ER and to the constantly blinking-out dilated ERESs. Using dual expression (Fig. 8A) of CFP- or YFP-tagged VSVG with Srβ-YFP, Sec13-YFP, Sec31-CFP, p58/ERGIC53-YFP and GRASP-65-DiHcRED, markers of ER, ERESs and Golgi membranes, we established that these are dilated ERES membranes that contain secretory and Golgi-targeted cargo proteins. Moreover, these membranes conducted a selective sorting process because they were devoid of the ER-membrane marker Srβ. Interestingly, the COPII markers did not evenly label the

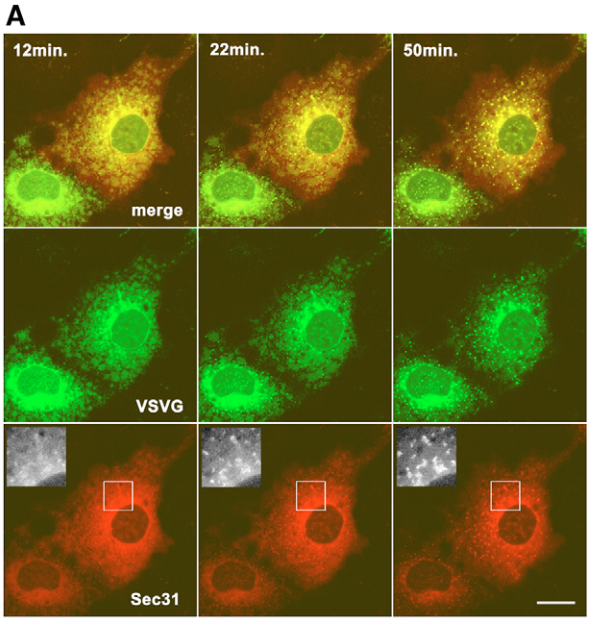

Fig. 5. Colocalization of VSVG-YFP and Sec31-CFP accumulation in ER exit site (ERES) membranes. (A) COS7 cells coexpressing VSVG-YFP (green) and Sec31-CFP (red) were treated as described in previous figures. Cells were transferred to the permissive temperature (34°C) and images were acquired at 2-minute intervals (see also supplementary material Movie 4). Scale bar: 10 μm. (B) Time-dependent increase in relative PFIVar of VSVG-YFP (green circles) and Sec31-CFP (red circles), calculated as described in the Materials and Methods, for the cell in A. Data were fitted to an exponential equation ($y = ae^{kx}$) (green and red lines for VSVG-YFP and Sec31-CFP, respectively). R^2 values were 0.98 and 0.97, and k values were 6.4 and 1.65% per minute, for VSVG and Sec31, respectively.

spherical ERES membranes but rather localized to a defined structure at a single distinct pole. To demonstrate that the selectivity of sorting is directly mediated by COPII, we eliminated it by mutagenesis of the Sec24-interacting acidic DIE motif at the cytosolic tail of VSVG-YFP to AIA (VSVG-YFP^{AIA}) (Nishimura et al., 1999). Fig. 8B clearly demonstrates that in the absence of the acidic motif, VSVG-YFP^{AIA} is excluded from the BFA-mediated spherical ERESs. These data show that VSVG-FP and other secretory cargo are actively and specifically sorted to ERES membranes in the absence of active COPI complex. Furthermore, these data also suggest that COPI and microtubules are essential for maintenance of the highly curved tubulovesicular structure of ERES membranes. Although the unique localization of COPII markers might be a result of the dependence of COPII dynamics on the presence of COPI and intact polymerized microtubules, its segregation from cargo has been reported (Mironov et al., 2003).

Our ability to obtain cargo sorting in the absence of microtubules and COPI prompted us to ask whether cholesterol depletion, shown to affect ER export (Ridsdale et al., 2006; Runz et al., 2006), would have an effect on the COPI- and microtubule-independent sorting. Cells expressing VSVG-FP were subjected to a 24 hour incubation in medium containing LDL-deficient serum and treated with methyl-β-cyclodextrin upon incubation with BFA and NOC on ice. Although cell morphology was significantly affected (Fig. 9A), VSVG-FP accumulated in the dilated ERESs. Analysis at the level of a single ERES showed a comparable yet somewhat slower rate of sorting (Fig. 9B).

In summary, we characterized the dynamics of the earliest sorting step of secretory transport in intact cells. Sorting and concentration of membrane cargo in ERESs was quantified directly in living cells by analyzing the time-dependent change in fluorescence-intensity variance after shift to the permissive temperature. The sorting process, measured in NOC-treated cells, was found to be slow and not limited by diffusion. Accumulation of cargo coincided with an increase in the ERES-bound CFP-tagged COPII component, Sec31. ER-to-ERES sorting and redistribution of VSVG-FP persisted in dilated ERES membranes devoid of ARF1, COPI and microtubules. Notably, these data exclusively assign the early sorting function to the COPII complex.

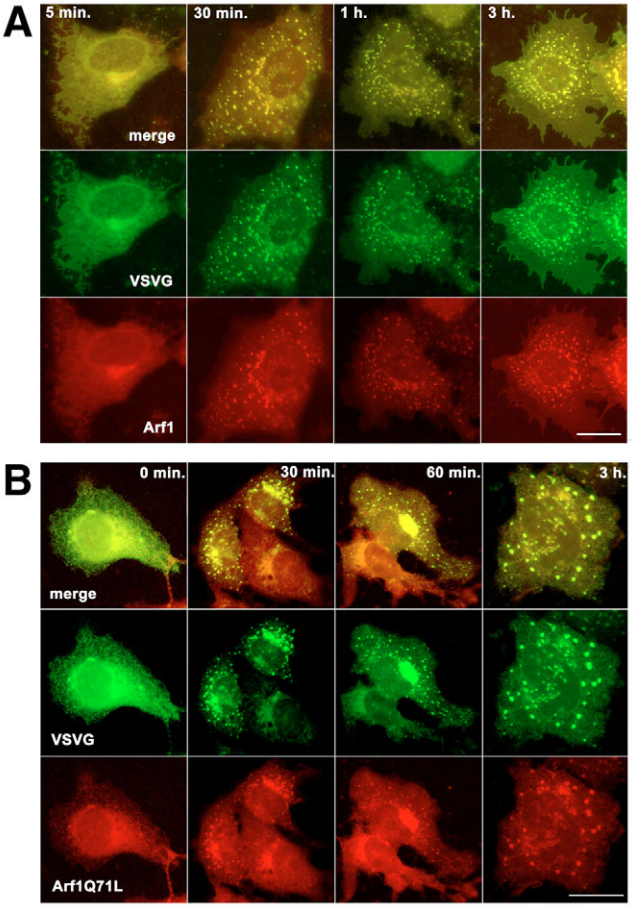

Fig. 6. Relationship between ARF1 and cargo-protein sorting to ER exit sites (ERESs). Confocal images of fixed COS7 cells coexpressing VSVG-YFP (green, A-B) and either the ARF1-CFP (A, red), or ARF1Q71L-CFP (B, red). Cells were transferred to ice for 20 minutes following a 24 hour incubation at the nonpermissive temperature (40°C). Nocodazole (1 μg/ml) was added, and the cells were returned for an additional 20 minutes to the nonpermissive temperature (40°C). After incubation at the permissive temperature (34°C) for the indicated times, cells were fixed by addition of 2% (v/v) formaldehyde and images were captured as described. Scale bars: 10 μm.

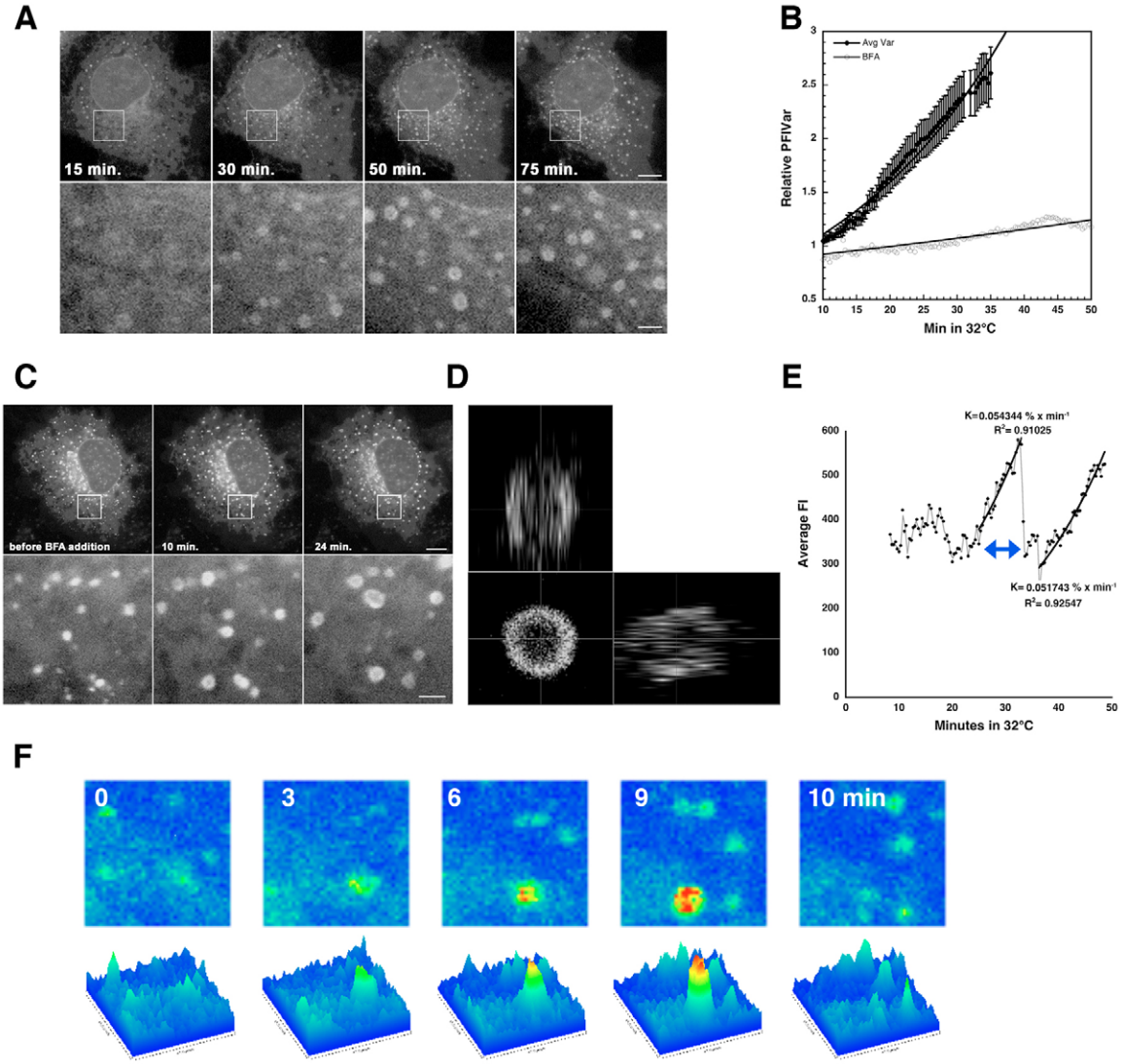

Fig. 7. Characterization of cargo concentration in brefeldin A (BFA) and nocodazole-induced dilated ER exit site (ERES) membranes. (A) Concentration of VSVG-FP in dilated membranes. COS7 cells, transfected with VSVG-FP, were shifted to the permissive temperature after overnight incubation at 39.5°C and 20 minutes at 4°C when 1 μg/ml nocodazole and 5 μg/ml BFA were added. Confocal images were captured at 20-second intervals (see supplementary material Movie 5). (B) Time-dependent increase in relative PFIVar of VSVG-YFP in the absence (average of 12 cells with s.e.m., filled circles) or presence (empty circles) of 5 μg/ml BFA, calculated as described in the Materials and Methods, for the cell in A. Data were fitted to an exponential equation ($y = ae^{kx}$) (green and red lines for VSVG-YFP and Sec31-CFP, respectively). R^2 values were 0.93 and 0.98, and k values were 3.64 and 0.74% per minute, for control and BFA-treated cells, respectively. (C) BFA was added 15 minutes after the shift to the permissive temperature (see supplementary material Movie 6). Scale bars: 20 μm. (D) Three-dimensional reconstruction of a confocal z-section series of a single dilated ERES. (E) Analysis of time-dependent average fluorescence intensity of a single dilated ERES during two cycles of cargo concentration and blink-out. The time zones including an increase in VSVG fluorescence were fitted separately to exponential equations (continuous lines). (F) Pseudocolor images (upper panel) and surface plot (lower panel) of the dilated ERES in E during the time labeled by the blue arrow in E.

Discussion

In this study, the redistribution and concentration dynamics of a membrane cargo protein was analyzed directly, in intact membranes of living cells. The sorting process counters the entropy-driven, even distribution of membrane proteins within organellar membranes. In the ER, cargo sorting is mediated by the ERES, which is a continuous albeit differentiated membrane domain with a characteristic protein and lipid composition. Thus, the ERES serves as a 'sink' that sorts cargo proteins (Balch et al., 1994). To isolate real-time information on the sorting of a fluorescently tagged cargo protein by the secretory machinery, the analysis was carried out in the absence of microtubules. This was necessary because lateral translocation of membrane carriers would have interfered with the acquisition of sorting information. Another advantageous outcome of microtubule depolymerization is the fact that the next secretory organelles in the transport pathway are superimposed on the ERESs. Thus transport from ERESs to VTCs and to the Golgi does not significantly affect the sorting information depicted by the PFIVar analysis. It should be noted that the later Golgi-to-plasma-membrane step does involve redistribution and dispersal of the fluorescent protein, which could affect the PFIVar analysis. However, the fluxes of Golgi-to-plasma membrane transport constitute less than 1% of the ER export fluxes during this time interval after the shift to the permissive

Table 1. Dimensions of dilated ERESs

	Without BFA	After BFA
Average diameter (μm)	0.684±0.15	1.025±0.22
Sphere volume (μm^3)	0.094	0.317
Surface area (μm^2)	*	5.88
Surface area/volume ratio (μm^{-1})	62.34	18.54

COS7 cells, transfected with FP-VSVG, were shifted to the permissive temperature after overnight incubation at 39.5°C. Nocodazole was added at the beginning of a 20-minute incubation at 4°C. The ERES diameter was measured from images captured 15 minutes after shift to permissive temperature as well as after an additional 30 minutes in the presence of BFA.

*We assume that the transformation of ERES to dilated ERES surface area does not change significantly compared with the luminal volume.

temperature (Hirschberg et al., 1998). The analysis of sorting in intact cells, using time-dependent changes in PFIVar, is also a straightforward and practical method to gain direct quantitative information on sorting of cargo proteins in the ER. This can be used as a functional assay to test the effect of various genetic and pharmaceutical perturbations in order to characterize the relationships among cargo-sorting signals, coat proteins and specific lipids. The relationship between the PFIVar values and the fold concentration in ERESs is not a simple one, because the variance does not measure concentration but rather the degree of spreading of pixel values around an average. The variance values depend on both the decrease in ER fluorescence values and the increase of VSVG-FP fluorescence in ERESs. Thus, in this system, the increase in variance values is, to a good approximation, linearly proportional to the increase in the distance between minimum and maximum pixel intensities.

The residence times of VSVG-GFP in the absence of NOC have been reported to be 39.4 and 42.0 minutes in the ER and Golgi complex, respectively (Hirschberg et al., 1998). In this study, the sorting analysis was carried out during the first 30-40 minutes after the temperature shift. Although the sorting and concentration of cargo is an early step that precedes budding and translocation on microtubule tracks, it is expected to be affected by a lack of polymerized microtubules in the cells, as characterized in Figs 1 and 2 (Watson et al., 2005). The dynamics of the sorting process is most likely altered as well, based on the finding that coat

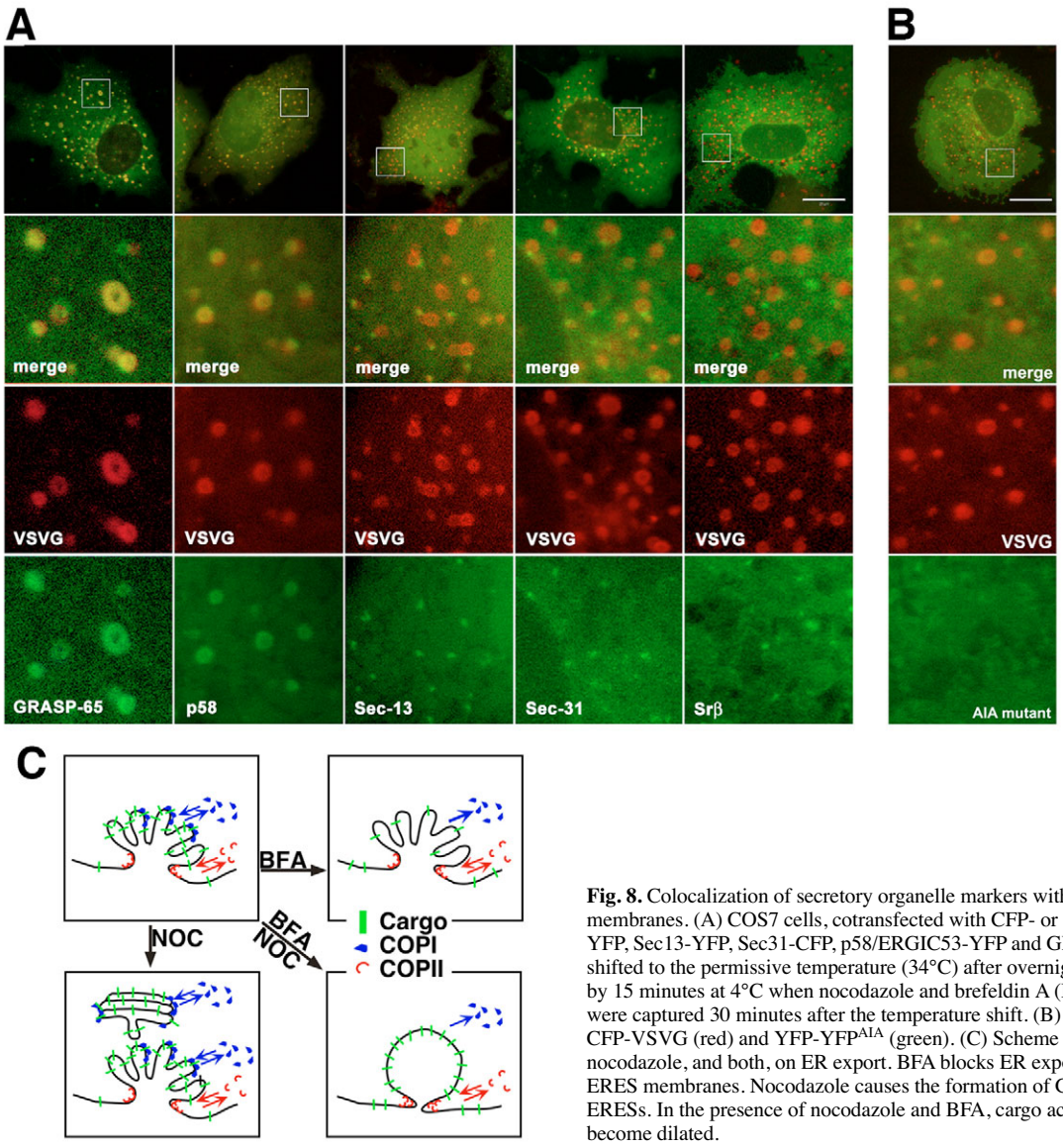

Fig. 8. Colocalization of secretory organelle markers with dilated ER exit site (ERES) membranes. (A) COS7 cells, cotransfected with CFP- or YFP-labeled VSVG (red) and Srβ-YFP, Sec13-YFP, Sec31-CFP, p58/ERGIC53-YFP and GRASP65-DiHcRED (green) were shifted to the permissive temperature (34°C) after overnight incubation at 39.5°C, followed by 15 minutes at 4°C when nocodazole and brefeldin A (BFA) were added. Confocal images were captured 30 minutes after the temperature shift. (B) COS7 cells were cotransfected with CFP-VSVG (red) and YFP-YFP^{AIA} (green). (C) Scheme depicting the effects of BFA, nocodazole, and both, on ER export. BFA blocks ER export and causes COPI release from ERES membranes. Nocodazole causes the formation of Golgi mini-stacks adjacent to the ERESs. In the presence of nocodazole and BFA, cargo accumulates in the ERESs, which become dilated.

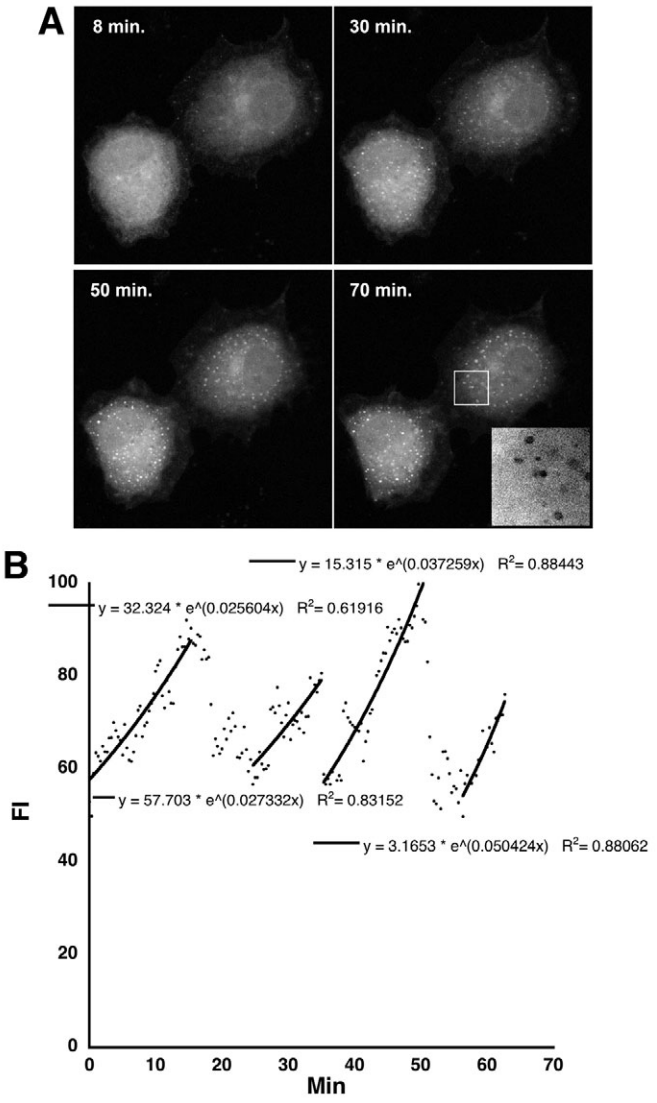

Fig. 9. Effect of cholesterol depletion on ER export in the presence of brefeldin A (BFA) and nocodazole. (A) COS7 cells, transfected with VSVG-FP, were shifted to the permissive temperature after overnight incubation at 39.5°C in medium containing LDL-deficient serum and 20 minutes at 4°C when 1 μg/ml nocodazole, 5 μg/ml BFA and 10 mM methyl-β-cyclodextrin were added. Confocal images were captured at 20-second intervals. (B) Analysis of time-dependent average fluorescence intensity (FI) of a single dilated ERES during several cycles of cargo concentration and blink-out in cholesterol-depleted cells. The time zones including an increase in VSVG fluorescence were fitted separately to exponential equations (continuous lines).

complexes interact with microtubules (Watson et al., 2005). In cells with intact microtubules, accumulation of VSVG-FP in ERESs is less apparent, since constantly budding ER-Golgi transport intermediates prevent its accumulation, as observed in NOC-treated cells. Thus, it can be inferred that the apparent rate of VSVG-FP sorting to ERESs reported here is probably slower than the normal rate of sorting in cells with intact microtubule tracks. Nevertheless, in a quantitative analysis of ER-export dynamics carried out for the same cell type and cargo molecules, the ER-residence times for the overall ER-to-Golgi transport process were reported to be 39.4±2.3 minutes (Hirschberg and Lippincott-Schwartz, 1999) or 20.4±1.9 minutes (Vasserman et al., 2006). Thus the time constants obtained in this study for sorting are comparable to those of ER export, which relate to all of the processes, i.e. sorting, budding and translocation to the Golgi complex. An attractive interpretation of these data is that in the ER, the sorting process is the rate-determining step for transport to the Golgi.

In Fig. 4, we show that the VSVG-FP cargo protein recycles back to the ER from compartments distal to ERESs. We propose that this recycling pathway can affect the relatively slow net sorting kinetics. We termed the sorting process as slow by comparison of its time constant with the time it takes a molecule to diffuse through an area that encloses a single ERES (area divided by the apparent diffusion coefficient of the VSVG-FP in ER membranes). However, we cannot rule out the possibility that sorting is limited by some other potentially slow process that precedes it, such as interaction with components of the ER folding and quality-control machinery. Analysis of the increase in VSVG-FP concentration at the level of a single ERES revealed complex kinetics in the form of a sigmoid-shaped curve. This can be interpreted as an indication of an initial delay or cooperative interactions at the initial stage of sorting, as well as some form of saturation at later stages that results from transport through superimposed successive organelles. Nevertheless, it is attractive to assume that the sigmoidal pattern reflects an increased rate of sorting because of cargo-dependent recruitment of COPII complexes to the ERES membranes. This is observed here for the COPII component Sec31 (Fig. 6), and elsewhere where cargo recruitment was shown to affect the turnover of COPII at ERESs (Forster et al., 2006).

Various lines of evidence support the hypothesis that sorting is mediated by multiple interactions. The VSVG-FP cargo contains at least two relevant targeting signals. The first is the DXE motif at the cytosolic tail (Nishimura et al., 1999; Votsmeier and Gallwitz, 2001), and the second is the transmembrane domain, the length of which has been shown to be a determinant for plasma membrane residence (Adams and Rose, 1985; Cole et al., 1998). Here we propose a model whereby the COPII coat complex directly selects cargo protein containing targeting signals (such as the DXE of VSVG), via transient interactions. COPII and COPI complexes also take part in the generation and maintenance of the appropriate physical state of the ERES membrane which, in turn, acts as a specific sink that thermodynamically stabilizes concentrated cargo destined for export. The co-incidence of COPII recruitment and cargo concentration suggests that the secretory machinery in ERESs is responsive to the amount of transported cargo, as has been previously reported (Guo and Linstedt, 2006). Sec31-CFP was also recruited in cells with intact microtubules (data not shown), suggesting that the recruitment is associated with the increase in cargo and is not a result of rearrangement of the Golgi complex.

Thus, in this study, the independent ability of COPII to actively and specifically sort cargo to ERESs is demonstrated, in accordance with previously published observations (Mezzacasa and Helenius, 2002). Our finding that COPII is localized to a distinct pole within the ERES that is segregated from most of the sorted cargo protein is also supported by published ultrastructural studies (Mironov et al., 2003). An attractive model that nevertheless requires further substantiation is that COPII defines the boundary of the ERES by forming transient cargo-dependent membrane-associated complexes (see scheme in Fig. 8C). Thus, entry into the ERES requires a sorting signal such as the DXE acidic motif of VSVG, to cross the COPII-coated boundary. Consequently, the transmembane domain may act as a secondary stabilizing entity that thermodynamically helps keep the selected cargo in place. This model predicts a possible directional

ratchet-like mode of function for the COPII complex that has yet to be verified. One possible prediction is that the COPII complex recruitment to the membrane and its polymerization occurs in a polarized fashion relative to the ERES-ER boundary.

The role of ARF1 GTPase and COPI in ER export is debatable, especially because COPI is considered to mediate transport in the opposite direction to that mediated by COPII. Several lines of evidence suggest a direct role for COPI in ER export (Bannykh et al., 2005; Barzilay et al., 2005; Ward et al., 2001). Here we found that sorting and concentration of cargo within ERESs proceed in cells overexpressing the membrane-locked, GTP-bound mutant form of ARF1 (Q71L), as well as in the presence of BFA. The mechanism underlying the combined effect of microtubule depolymerization and the presence of BFA, whereby ERES membranes transform to a sphere, is not clear. However, it sheds light on the distinct roles within the sequential function of COPI and COPII complexes in ER export (Scales et al., 1997). One explanation for the ability of VSVG-FP and other cargo proteins (Fig. 8) to be sorted to ERESs in the absence of COPI and microtubules is that membrane cargo proteins can spontaneously sort into COPII-containing export domains. The Arf1 GTPase and COPI complex associate with microtubules to regulate and facilitate this intrinsic capability by stabilizing concentrated cargo-containing membranes.

The fact that the formation of dilated ERES membranes is associated with BFA and NOC implies a fundamental role for COPI and microtubules in imposing the highly curved tubulovesicular structure of the ERES membranes (see scheme in Fig. 8C). Moreover, the ongoing concentration of cargo in the dilated membranes demonstrates that COPI- and microtubule-mediated membrane curvature is not stringently essential for cargo sorting. Thus, it may be that the ERES membrane curvature is important in determining the efficiency and extent of this process. Also, the highly curved membranes may serve to maintain a high membrane surface-area-to-volume ratio, for example, to minimize loss via the exchange of luminal contents, or to increase the efficiency of transport-coupled enzymatic modifications. The frequent fusion of the cargo-containing spherical membranes with the ER indicates that the cargo-protein-enriched but Arf1- and COPI-depleted membranes are unstable. It is possible that a direct outcome of COPI binding is the blockage of such spontaneous fusion events, as previously suggested (Ostermann et al., 1993).

Finally, cargo sorting and concentration are fundamental yet enigmatic functions of the intracellular transport machinery. We propose that the ERES acts as a specific sink for transport-competent cargo proteins. The kinetics and dynamics of the sorting process are suggestive of an important role for cargo-coat complex (COPII) recognition as well as for the membrane lipids. Thus, the relationships within the triangle of cargo-targeting signals, membrane and coat complexes is only beginning to be unraveled. Analysis of these processes requires innovative approaches that utilize the intact cell membrane as the central experimental arena, thereby taking its complexity and dynamics into consideration.

Materials and Methods

Reagents and constructs

All reagents were purchased from Sigma Chemical Co. (St Louis, MO) unless otherwise stated. Srβ-CFP was a kind gift from the laboratory of R.S. Hegde (Snapp et al., 2006). GPI-mCFP was from the laboratory of B. Nichols (Glebov and Nichols, 2004). VSVGtsO45-YFP was prepared as described elsewhere (Ward et al., 2001). Sec31-CFP was a kind gift from R. Pepperkok (Stephens et al., 2000) and ARF1-CFP and ARF1Q71L were from the laboratory of J. Lippincott-Schwartz (Presley et al., 2002). VSVGtsO45-YFP^{AIA} was prepared using the Quik-Change kit from Stratagene (La Jolla, CA). The primer used for the PCR reaction was 5′-GACAGATTTATACAGCCATAGCGATGAACCGAC-3′.

Cell culture and transient transfection

COS7 cells (African green monkey) were grown at 37°C in a humidified atmosphere with 5% CO_2. Cell cultures were maintained in Dulbecco's modified Eagle's medium (DMEM) supplemented with 10% (v/v) fetal bovine serum (FBS) and penicillin/streptomycin (Biological Industries, Bet-Haemek, Israel). For microscopy, cells were subcultured in glass coverslip chambers (Nalgene Nunc, Rochester, NY), grown to 20-30% confluence and then transiently transfected with 1.5 μg DNA/chamber using FuGENE-6 reagent (Roche Applied Science, Mannheim, Germany). Cholesterol depletion was carried out by an overnight incubation of the cells with medium containing lipoprotein-deficient fetal calf serum (Sigma, St Louis, MO). Prior to the experiment, methyl-β-cyclodextrin (10 mM) was added to the medium.

Confocal laser-scanning microscopy

Cells were imaged in DMEM without Phenol Red but with supplements, including 20 mM HEPES, pH 7.4. Transfection and imaging were carried out in Labtek chambers (Nunc). A Zeiss LSM PASCAL (Carl Zeiss MicroImaging, Jena, Germany) was equipped with an Axiovert 200 inverted microscope, and Ar 458 nm, 488 nm and 514 nm laser lines for ECFP, EGFP and EYFP, respectively. The confocal and time-lapse images were captured using a Plan-Apochromat 63× NA 1.4 objective (Carl Zeiss MicroImaging). Image capture was carried out using the standard time-series option (Carl Zeiss MicroImaging). Temperature on the microscope stage was monitored during time-lapse sessions using an electronic temperature-controlled airstream incubator. Images and movies were generated and analyzed using the Zeiss LSM software, NIH Image and ImageJ software (W. Rasband, NIH, Bethesda, MD).

Confocal LSM, time-lapse imaging, fluorescence recovery after photobleaching analysis and image processing

Long time-lapse image sequences were captured using the autofocusing function integrated into the 'advanced time series' macro set (Carl Zeiss MicroImaging). For quantitative FRAP measurements, a 63× 1.4 NA Plan-Apochromat objective was used. Photobleaching of GFP or YFP was performed as described here or using 4-6 scans with the 488 nm laser line at full power in the 8-μm-wide rectangular ROI. Pre- and post-bleach images were captured at 2- to 5-second intervals, using low laser intensity, by capturing a ROI around the bleach box. Fluorescence recovery in the bleached region during the time series was quantified using LSM software (Carl Zeiss MicroImaging). For presentation purposes, confocal images were exported in TIFF and their contrast and brightness optimized in Adobe Photoshop (San Jose, CA). D values were calculated from the photobleaching data using a fit to an approximate solution of the diffusion equation when the elongated rectangular bleach box has a width a, which is much smaller than its length. According to this solution, the fluorescence intensity in the bleach box at time t, F_t, can be presented as:

$$F_t = M_f\left(1 + Ae^{-\left[\frac{1D\pi}{a^2}t\right]} - (1+A)\,e^{-\left[\frac{9D\pi}{a^2}t\right]}\right),$$

where M_f is the mobile fraction, D is the diffusion coefficient and A serves as a second fitting parameter. Time-dependent changes in fluorescence intensity in the bleach box were normalized to pre-bleach and post-bleach values of 1 and 0, respectively. Data were then fitted to the above equation using Kalaidagraph (Synergy software, Essex-Junction, VT). PFIVar values, analysis and surface plots of single ERES fluorescence intensities were calculated using ImageJ (Wane Rasband, NIH, Bethesda, MD). The values were normalized by dividing all variance values by the initial one (at t=0). The photobleaching experiments were carried out using SAAM II software (Univ. of Washington, Seattle, WA). The experiment was simulated using a two-compartment model with one flux delineating VSVG-FP movement from the unbleached to the bleached ROI.

We would like to thank Michael Kozlov for fruitful discussions and for providing the equation for the FRAP experiments. We also thank R. Pepperkok (EMBL), B. Nichols (MRC), J. Lippincott-Schwartz (NIH) and E. Snapp (NIH) for the various expression plasmids. This work was funded in part by BSF grant #2005281 to K.H. A.P. is funded in part by the EU Marie Curie Research Training Network on Flipases.

References

Adams, G. A. and Rose, J. K. (1985). Structural requirements of a membrane-spanning domain for protein anchoring and cell surface transport. *Cell* **41**, 1007-1015.

Antonny, B. (2006). Membrane deformation by protein coats. *Curr. Opin. Cell Biol.* **18**, 386-394.

Balch, W. E., McCaffery, J. M., Plutner, H. and Farquhar, M. G. (1994). Vesicular stomatitis virus glycoprotein is sorted and concentrated during export from the endoplasmic reticulum. *Cell* **76**, 841-852.

Bannykh, S. I., Plutner, H., Matteson, J. and Balch, W. E. (2005). The role of ARF1 and rab GTPases in polarization of the Golgi stack. *Traffic* **6**, 803-819.

Barzilay, E., Ben-Califa, N., Hirschberg, K. and Neumann, D. (2005). Uncoupling of brefeldin a-mediated coatomer protein complex-I dissociation from Golgi redistribution. *Traffic* **6**, 794-802.

Cole, N. B., Sciaky, N., Marotta, A., Song, J. and Lippincott-Schwartz, J. (1996). Golgi dispersal during microtubule disruption: regeneration of Golgi stacks at peripheral endoplasmic reticulum exit sites. *Mol. Biol. Cell* **7**, 631-650.

Cole, N. B., Ellenberg, J., Song, J., DiEuliis, D. and Lippincott-Schwartz, J. (1998). Retrograde transport of Golgi-localized proteins to the ER. *J. Cell Biol.* **140**, 1-15.

Dascher, C. and Balch, W. E. (1994). Dominant inhibitory mutants of ARF1 block endoplasmic reticulum to Golgi transport and trigger disassembly of the Golgi apparatus. *J. Biol. Chem.* **269**, 1437-1348.

Forster, R., Weiss, M., Zimmermann, T., Reynaud, E. G., Verissimo, F., Stephens, D. J. and Pepperkok, R. (2006). Secretory cargo regulates the turnover of COPII subunits at single ER exit sites. *Curr. Biol.* **16**, 173-179.

Fromme, J. C. and Schekman, R. (2005). COPII-coated vesicles: flexible enough for large cargo? *Curr. Opin. Cell Biol.* **17**, 345-352.

Glebov, O. O. and Nichols, B. J. (2004). Distribution of lipid raft markers in live cells. *Biochem. Soc. Trans.* **32**, 673-675.

Graham, T. R. (2004). Membrane targeting: getting Arl to the Golgi. *Curr. Biol.* **14**, R483-R485.

Guo, Y. and Linstedt, A. D. (2006). COPII-Golgi protein interactions regulate COPII coat assembly and Golgi size. *J. Cell Biol.* **174**, 53-63.

Hirschberg, K. and Lippincott-Schwartz, J. (1999). Secretory pathway kinetics and in vivo analysis of protein traffic from the Golgi complex to the cell surface. *FASEB J.* **13** Suppl. 2, S251-S256.

Hirschberg, K., Miller, C. M., Ellenberg, J., Presley, J. F., Siggia, E. D., Phair, R. D. and Lippincott-Schwartz, J. (1998). Kinetic analysis of secretory protein traffic and characterization of golgi to plasma membrane transport intermediates in living cells. *J. Cell Biol.* **143**, 1485-1503.

Hobman, T. C., Zhao, B., Chan, H. and Farquhar, M. G. (1998). Immunoisolation and characterization of a subdomain of the endoplasmic reticulum that concentrates proteins involved in COPII vesicle biogenesis. *Mol. Biol. Cell* **9**, 1265-1278.

Lippincott-Schwartz, J., Roberts, T. H. and Hirschberg, K. (2000). Secretory protein trafficking and organelle dynamics in living cells. *Annu. Rev. Cell Dev. Biol.* **16**, 557-589.

Mezzacasa, A. and Helenius, A. (2002). The transitional ER defines a boundary for quality control in the secretion of tsO45 VSV glycoprotein. *Traffic* **3**, 833-849.

Miller, E. A., Beilharz, T. H., Malkus, P. N., Lee, M. C., Hamamoto, S., Orci, L. and Schekman, R. (2003). Multiple cargo binding sites on the COPII subunit Sec24p ensure capture of diverse membrane proteins into transport vesicles. *Cell* **114**, 497-509.

Mironov, A. A., Mironov, A. A., Jr, Beznoussenko, G. V., Trucco, A., Lupetti, P., Smith, J. D., Geerts, W. J., Koster, A. J., Burger, K. N., Martone, M. E. et al. (2003). ER-to-Golgi carriers arise through direct en bloc protrusion and multistage maturation of specialized ER exit domains. *Dev. Cell* **5**, 583-594.

Mossessova, E., Corpina, R. A. and Goldberg, J. (2003). Crystal structure of ARF1*Sec7 complexed with Brefeldin A and its implications for the guanine nucleotide exchange mechanism. *Mol. Cell* **12**, 1403-1411.

Nehls, S., Snapp, E. L., Cole, N. B., Zaal, K. J., Kenworthy, A. K., Roberts, T. H., Ellenberg, J., Presley, J. F., Siggia, E. and Lippincott-Schwartz, J. (2000). Dynamics and retention of misfolded proteins in native ER membranes. *Nat. Cell Biol.* **2**, 288-295.

Nishimura, N., Bannykh, S., Slabough, S., Matteson, J., Altschuler, Y., Hahn, K. and Balch, W. E. (1999). A di-acidic (DXE) code directs concentration of cargo during export from the endoplasmic reticulum. *J. Biol. Chem.* **274**, 15937-15946.

Ostermann, J., Orci, L., Tani, K., Amherdt, M., Ravazzola, M., Elazar, Z. and Rothman, J. E. (1993). Stepwise assembly of functionally active transport vesicles. *Cell* **75**, 1015-1025.

Presley, J. F., Cole, N. B., Schroer, T. A., Hirschberg, K., Zaal, K. J. and Lippincott-Schwartz, J. (1997). ER-to-Golgi transport visualized in living cells. *Nature* **389**, 81-85.

Presley, J. F., Ward, T. H., Pfeifer, A. C., Siggia, E. D., Phair, R. D. and Lippincott-Schwartz, J. (2002). Dissection of COPI and Arf1 dynamics in vivo and role in Golgi membrane transport. *Nature* **417**, 187-193.

Ridsdale, A., Denis, M., Gougeon, P. Y., Ngsee, J. K., Presley, J. F. and Zha, X. (2006). Cholesterol is required for efficient endoplasmic reticulum-to-Golgi transport of secretory membrane proteins. *Mol. Biol. Cell* **17**, 1593-1605.

Rogalski, A. A., Bergmann, J. E. and Singer, S. J. (1984). Effect of microtubule assembly status on the intracellular processing and surface expression of an integral protein of the plasma membrane. *J. Cell Biol.* **99**, 1101-1109.

Runz, H., Miura, K., Weiss, M. and Pepperkok, R. (2006). Sterols regulate ER-export dynamics of secretory cargo protein ts-O45-G. *EMBO J.* **25**, 2953-2965.

Scales, S. J., Pepperkok, R. and Kreis, T. E. (1997). Visualization of ER-to-Golgi transport in living cells reveals a sequential mode of action for COPII and COPI. *Cell* **90**, 1137-1148.

Sciaky, N., Presley, J., Smith, C., Zaal, K. J., Cole, N., Moreira, J. E., Terasaki, M., Siggia, E. and Lippincott-Schwartz, J. (1997). Golgi tubule traffic and the effects of brefeldin A visualized in living cells. *J. Cell Biol.* **139**, 1137-1155.

Siggia, E. D., Lippincott-Schwartz, J. and Bekiranov, S. (2000). Diffusion in inhomogeneous media: theory and simulations applied to whole cell photobleach recovery. *Biophys. J.* **79**, 1761-1770.

Snapp, E. L., Sharma, A., Lippincott-Schwartz, J. and Hegde, R. S. (2006). Monitoring chaperone engagement of substrates in the endoplasmic reticulum of live cells. *Proc. Natl. Acad. Sci. USA* **103**, 6536-6541.

Stephens, D. J., Lin-Marq, N., Pagano, A., Pepperkok, R. and Paccaud, J. P. (2000). COPI-coated ER-to-Golgi transport complexes segregate from COPII in close proximity to ER exit sites. *J. Cell Sci.* **113**, 2177-2185.

Storrie, B., White, J., Rottger, S., Stelzer, E. H., Suganuma, T. and Nilsson, T. (1998). Recycling of golgi-resident glycosyltransferases through the ER reveals a novel pathway and provides an explanation for nocodazole-induced Golgi scattering. *J. Cell Biol.* **143**, 1505-1521.

Tang, B. L., Wang, Y., Ong, Y. S. and Hong, W. (2005). COPII and exit from the endoplasmic reticulum. *Biochim. Biophys. Acta* **1744**, 293-303.

Vasserman, G., Magal, L. G., Shepshelovich, J., Elifaz, E. and Hirschberg, K. (2006). Processing of VSVG protein is not a rate-limiting step for its efflux from the Golgi complex. *Biochem. Biophys. Res. Commun.* **351**, 689-694.

Voeltz, G. K., Rolls, M. M. and Rapoport, T. A. (2002). Structural organization of the endoplasmic reticulum. *EMBO Rep.* **3**, 944-950.

Votsmeier, C. and Gallwitz, D. (2001). An acidic sequence of a putative yeast Golgi membrane protein binds COPII and facilitates ER export. *EMBO J.* **20**, 6742-6750.

Ward, T. H., Polishchuk, R. S., Caplan, S., Hirschberg, K. and Lippincott-Schwartz, J. (2001). Maintenance of Golgi structure and function depends on the integrity of ER export. *J. Cell Biol.* **155**, 557-570.

Watson, P., Forster, R., Palmer, K. J., Pepperkok, R. and Stephens, D. J. (2005). Coupling of ER exit to microtubules through direct interaction of COPII with dynactin. *Nat. Cell Biol.* **7**, 48-55.